ISSN: 2449 - 0539
BAYERO JOURNAL OF ENGINEERING AND TECHNOLOGY VOL. 18 NO. 2 MAY 2023 PP. 95-103

ENHANCEMENT OF RECEIVED POWER DISTRIBUTION OF A NON-DIRECTED LoS INDOOR VISIBLE LIGHT COMMUNICATION SYSTEM

[1]S.F. Kolawole, [2]M. Hamza

[1]Department of Electrical and Electronics Engineering, Nigeria Defence Academy, Kaduna

[2]Department of Electrical and Electronics Engineering, Kaduna Polytechnic, Kaduna.

[1]sfkolawole@nda.edu.ng [2]hamzamusa@kadunapolytechnic.edu.ng

ABSTRACT

Visible light communication uses the visible light portion of the electromagnetic spectrum to achieve communication with light as the carrier of information and optical power is received at the receiver. The received power distribution uniformity may sometimes be inefficient or traded off with maximum received power, this problem then inhibits communication quality in a receiving plane for visible light communication in an indoor environment due to power fluctuation. A novel way of arranging 9 transmitters is presented in this work based on non-direction line of sight VLC. The Visible light communication system for an indoor environment here is hence, both in terms of line of sight and non light of sight scenarios. Using a model of VLC system which includes the transmitter, receiver, room and signal propagation, the received power is simulated jointly for both scenarios to produce a received power distribution across a communication environment. The simulations were carried out considering two separate 9-transmitters configurations of which one is a conventional arrangement and the other is the novel arrangement presented in this work. MATLAB was used for the simulations and the results were compared and analysed. The novel transmitter configuration was found to have better received power distribution by 9% without diminishing the maximum received power where there is high probability of having a receiver. The maximum received power was actually even improved from 2.38 mW to 2.44 mW. The results of the novel configuration can lead to reduction in power fluctuation within a communication environment and improve mobility.

Keywords: distribution uniformity; novel configuration; received power; signal propagation; indoor VLC.

1. INTRODUCTION

Visible light communication (VLC) has become a promising candidate to complement conventional RF communication especially with the rapid increase in demand for wireless data access and the saturation of the radio frequency spectrum (Yu et al., 2013). According to CISCO, globally, the total number of internet users is expected to grow from 3.9 billion in 2018 to 5.3 billion in this year 2023 (CISCO, 2020).

Visible light communication (VLC) refers to the communication technology which utilizes the visible light source (usually LED) as a signal transmitter, the free space as a transmission medium, and the appropriate photodiode as a signal receiving component (Lee, 2011). In VLC, the lighting sources (LEDs) actually have a primary functionality of serving as illumination sources, it is these lighting sources that are now designed with VLC capabilities for communication use.

The transmitter could modulate LEDs at very high frequencies to appear invariant as perceived by human eyes (Cheng et al., 2018). As the LED is modulated at the frequency higher than the response of human eye, the eye cannot experience light flashing (Wang et al., 2017). This brings about the attractive dual usage of the LED as a source of light for illumination and also for communication.

Among several other advantages compared to RF systems, LED transmitters offer higher data transmission at rates comparable to fiber optics with a fraction of its deployment cost (Slaiman et al., 2014). The rest of this paper is organized as follows; section two discusses review of past works, section three details the system model, section four presents the simulation, results and analysis. Section five covers the conclusion and section recommendations for future work.

2. LITERATURE REVIEW

A study on the effect of LEDs position for an indoor environment on the performance of a VLC system was provided in (Khalifeh et al., 2019), considering only the LoS link where it was shown that different arrangements of the LED transmitters affects the amount of power received at the photodetector. The authors used 4 and 9 transmitter arrays and were able to show that for the 4
transmitters array, there was a high fluctuation between peak received power and the minimum received power. The 9 transmitter array was then used to achieve better distribution and it was shown that widening the gap between the transmitters improve power distribution although at the cost of reduced peak power.

A research on optimization of received power and SNR was presented in (Gismalla & Abdullah, 2019) where the authors proposed a novel indoor attocells (VLC base station/LED) network configuration model to optimize received power and SNR in visible light communication, the proposed model was applied for just the indoor LoS links. They used 5 attocell model and compared their work with 4 attocells model where simulation results showed that their proposed model saves transmitted power and improves coverage area but requires additional attocells to achieve this.

In the work of (Abdelrahman & Abdulwahab, 2019), a research was conducted to enhance SNR and optical power distribution in indoor visible light communications systems where the authors found optimum uniformity between three scenarios of transmitter arrangement using 4 LEDs. All the LEDs were located on the orthogonal axes of the room and they considered the LoS link separately from the diffuse link. Through simulations, they were able to find the arrangement with a better optical power distribution and high SNR than other configurations.

An investigation on optimized LEDs positions for channel analysis performance of an intra-vehicle visible light communication system was conducted by (Shaaban & Faruque, 2020). The main aim of the paper was to optimize the LEDs positioning and allocation and notice how they affect the system design and performance. The authors first employed a 2 source models and then a 3 source models to increase power but at increased cost, this 3 source models were then optimized for better power distribution.

A research was carried out on improved uniformity for an indoor visible light communication system in terms of high received power and SNR by (Gismalla et al., 2020). The paper featured a novel model configuration using 13 attocells (LEDs). They compared their proposed work with a topology from other works that utilised 4 and 16 LEDs at the same number of sub-arrays, they however, varied the field of view (FOV). Their topology was seen to provide better uniformity of distribution of power.

A transmitter half distribution angle optimization scheme was provided by (Sekaran et al.,2022) in order to improve received power at the receiver in non line of sight VLC and minimize spatial power fluctuation. The authors sought to maximise received power through non line of sight due its resilience to blocking, hence they considered only the non line of sight aspect of VLC.

This work is carried out to enhance the received power distribution of visible light communication in the indoor environment for a 9 transmitter configuration considering a non directed LoS link.

3. METHDOLOGY

The methodology of this work presents the modeling of the entire VLC system as a non-directed LoS link, it also covers the arrangement of the LED transmitters in terms of both the conventional 9 transmitters arrangement and the novel 9 transmitters arrangement proposed in this work. The link geometry for the directed LoS is given in *figure 1* while the link geometry for the reflected link is shown in *figure 2*. Based on the consideration of non-directed LoS link, The system model is based on these 2 link geometries in a communication environment for visible light communication.

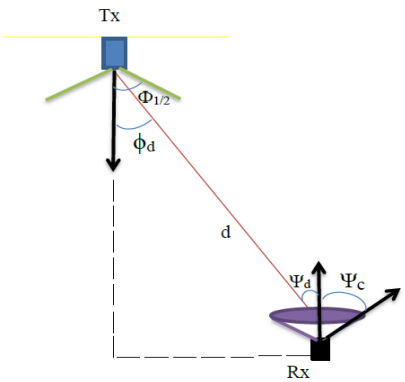

Figure 1: Geometry of directed (LoS) link between transmitter and receiver

Where $\Phi_{1/2}$ is transmitter half power angle, ϕ_d is angle of irradiance from transmitter, d is distance between transmitter and receiver, ψ_d is angle of incidence on receiver,ψ_c is receiver FOV, Tx is transmitter and Rx is receiver.

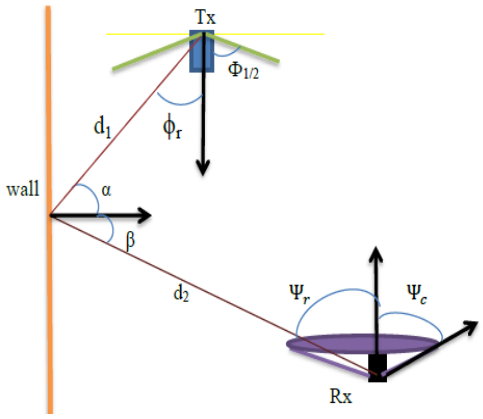

Figure 2: Geometry of reflected (diffuse) link between transmitter and receiver

Where $\Phi_{1/2}$ is LED half power angle, ϕ_r is the angle of irradiance, α is the angle of incidence on reflective point, β is the angle of irradiance from a reflective point,ψ_r is the angle of incidence on the receiver, ψ_c is the FOV of

receiver, d_1 is the distance from transmitter to reflective point, d_2 is the distance from reflective point to receiver, Tx is transmitter and Rx is receiver.

3.1 Transmitter, Receiver and Room

The Transmitter is assumed to have a Lambertian radiation pattern as its light distribution and is modeled using the Lambertian radiant intensity which is given from (Dawoud et al., 2020) as;

$$R(\phi) = \frac{(m_l+1)}{2\pi} cos^{m_l}(\phi) \quad . \ . \ . \quad (1)$$

Where ϕ is the angle of irradiance from transmitter. m_l is Lambert's mode number which gives directivity of the light from source. It is related to the half power angle of transmitter as shown in eqn. (2) where the order of m_l is given as (Dawoud et al., 2020);

$$m_l = \frac{-\ln(2)}{\ln(\cos \Phi_{1/2})} \quad . \ . \ . \quad (2)$$

Where $\Phi_{1/2}$ is the transmitter half power angle.

If A_a is the physical area of the receiver, and ψ is the angle of incidence on the receiver, then the effective area A_c that the photodetector will use to collect incoming light is given by;

$$A_c = A_a \cos \quad . \ . \ . \quad (3)$$

If the receiver field of view (FOV) is considered (light cannot be captured outside this field) and an optical concentrator and optical filter are used to improve the receiver performance, the effective area A_c becomes;

$$A_c(\psi) = \begin{cases} A_a \cos\psi \times G(\psi) \times T(\psi), & for\ 0 \le \psi \le \psi_c \\ 0, & for\ \psi > \psi_c \end{cases} \quad \ldots \quad (4)$$

Where ψ_c is the receiver FOV, $T(\psi)$ is the gain of optical filter and $G(\psi)$ is the optical concentrator gain. The gain of the optical concentrator from (Mulyawan et al., 2017) is given as;

$$G(\psi) = \frac{n^2}{sin^2\psi_c} \quad . \ . \ . \quad (5)$$

Where n is internal refractive index of the material used.

3.2 Signal Propagation Model

The signal propagation in VLC includes both the LoS and the reflected components and both are considered in this work. Based on the geometry of the LoS link in *figure 1* and the transmitter and receiver models, the channel DC gain of the LoS link $H_{los}(O)$ is given as (Vatansever et al., 2017)

$$H_{los}(O) = \begin{cases} \frac{(m_l+1)}{2\pi d^2} A_a cos^{m_l}(\phi_d) T(\psi_d) G(\psi_d) cos(\psi_d), & for\ 0 \le \psi_d \le \psi_c \\ 0, & elsewhere \end{cases} \quad \ldots \quad (6)$$

Where $\Phi_{1/2}$ is transmitter half power angle, ϕ_d is angle of irradiance from transmitter, d is distance between transmitter and receiver, ψ_d is angle of incidence on receiver, A_a is physical area of receiver, ψ_c is receiver FOV, $T(\psi_d)$ is optical filter gain, $G(\psi_d)$ is gain of optical concentrator.

The light transmitted from source may undergo several number of reflections, the channel dc gain for the desired number of reflections can be obtained recursively. However, in this work, due to complexity and computation time, only the first order of reflection is considered. Therefore, considering the geometry in *figure 2* and relating it to the geometry and channel dc gain of the LoS link, the reflected link channel will be a result of 2 components. First component is from transmitter to the wall surface, where the wall is considered to be a receiver, the second component is from wall surface to the main receiver whereby in this case, the wall is considered to be a transmitter. The 2 components in isolation can be considered to be a

direct line of sight link but their combination gives the reflected link channel dc gain $H_{ref}(O)$ as given by (Madani et al., 2017);

$$H_{ref}(O) = \begin{cases} \frac{(m_l+1)}{2(\pi d_1 d_2)^2}\rho \times A_a \times dA_w \times cos^{m_l}(\phi_r) \times cos(\alpha) \times cos(\beta) \times \\ \quad cos(\psi_r) \times T(\psi_r) \times G(\psi_r), \quad for\ 0 \le \psi_r \le \psi_c \quad \ldots (7) \\ 0, \quad elsewhere \end{cases}$$

where $\Phi_{1/2}$ is LED half power angle, ϕ_r is the angle of irradiance from transmitter, α is the angle of incidence on reflective point on wall, β is the angle of irradiance from the reflective point, ψ_r is the angle of incidence on the receiver, ψ_c is the FOV of receiver, $T(\psi_r)$ is the gain of optical filter, $G(\psi_r)$ is gain of optical concentrator, A_a is physical area of receiver, ρ is wall reflectivity, dA_w is reflective area, d_1 is the length from transmitter to reflective point, d_2 is the distance from reflective point to receiver.

The dimensions of an ISO (International Organisation for Standardization) specified standard office environment of size $L_x \times L_y \times L_z = 5m \times 5m \times 3m$ is adopted as the indoor communication environment. The 3D depiction in *figure 3* illustrates the office environment showing the various lengths and communication links. The receiver is chosen to be placed at a standard table top height of $0.85m$ denoted by r while s is now the effective communication height.

$s = L_z - r = 3m - 0.85m = 2.15m.$

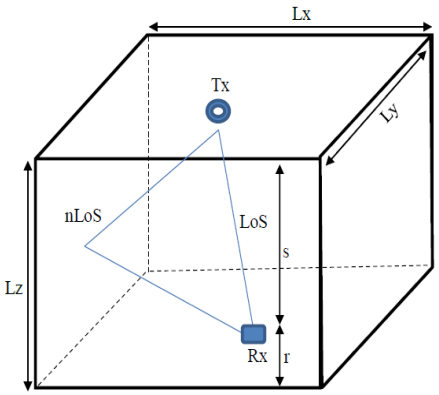

Figure 3: Complete VLC Model in an indoor communication space showing transmitter (Tx) on ceiling, receiver (Rx), line of sight link(LoS) and reflected link (nLoS).

3.3 Transmitter Configuration

The conventional way of placing 9 lighting points is mostly to have them in an array of 3×3 configuration. These lighting points are the transmitters in VLC. The easiest way to improve the power distribution of the 9 transmitters in a 3×3 array is by placing them farther away from each other and taking them closer to the wall sides as shown in (Khalifeh et al., 2019). However, this then diminishes the peak received power at center, hence improving the distribution comes at the cost of decreasing maximum power and vice versa. This leads to the adoption of a certain 3×3 array whereby the transmitters will have equal spacing and also equal distances away from the wall, this offers a middle ground. The transmitter placement coordinates on the ceiling corresponding to this arrangement is $x(m)\_(-1.25, 0, 1.25)$ and $y(m)\_(-1.25, 0, 1.25)$ and this is shown in *figure 4*.

The novel configuration which is shown in *figure 5* presents a different approach by proposing an entirely different arrangement, this arrangement is further designed to be at distances that improve the received power distribution without diminishing the peak received power where there is high probability of having a receiver in office setting. The transmitter placement coordinates on the ceiling corresponding to this arrangement is $\{[x(m)\_(-2,2)$ and $y(m)\_(-1.66,1.66)]$, $[x(m)\_(-0.417, 0.417)$ and $y(m)\_(-0.625, 0.625)]$, $[x(m)\_(0)$ and $y(m)\_(0)]\}$.

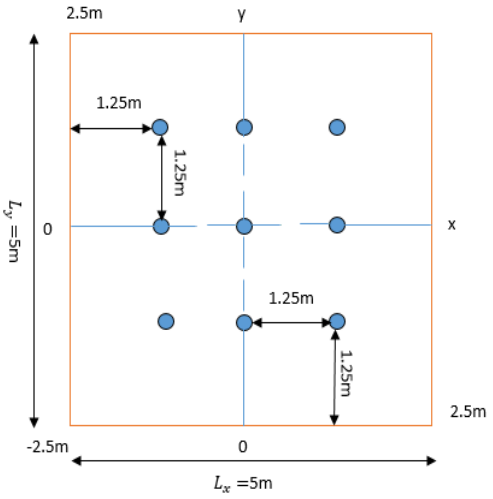

***Figure 4*:** Conventional configuration

ISSN: 2449 - 0539
BAYERO JOURNAL OF ENGINEERING AND TECHNOLOGY VOL. 18 NO. 2 MAY 2023 PP. 95-103

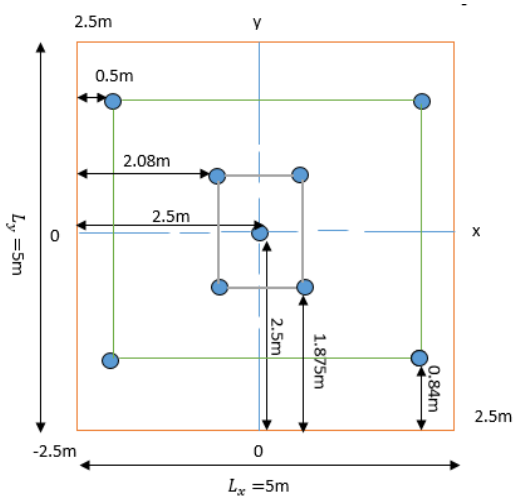

***Figure 5*: Novel configuration**

3.4 Received Power

The total power received by the receiver is a result of the two links, directed LoS and reflected link. For a total transmitted power P_{total}, the received power P_r is as given by (Chvojka et al., 2015);

$$P_r = P_{total}H_{los}(0) + P_{total}H_{ref}(0) \quad . \ . \ . \quad (8)$$

Since the main reflections are coming from the wall surfaces and there are 4 walls in a room, P_r can be rewritten as;

$$P_r = P_{total}H_{los}(0) + P_{total}\sum_{ref=1}^{4} H_{ref}(0) \quad . \ . \ . \quad (9)$$

Where the reflected portion of the received power is now a summation over the 4 walls.
For the multiple optical sources, that is the 9 transmitters, eqn. (9) becomes;

$$P_r = \sum_{i=1}^{9}\left(P_{total}(H_{los}(0) + P_{total}\sum_{ref=1}^{4} H_{ref}(0)\right) \ . \ . \ . \quad (10)$$

The equation obtained in eqn. (10) can generally be applied to any 9 transmitter configuration that is considering only 1 reflection. For the novel configuration in this work which is given in *figure 5*, the received power is broken down to conform to the 3 layers in the arrangement. eqn. (10) is rewritten as 3 parts summation which are for the double 2 × 2 array and the single point source transmitter.

$$P_r = \sum_{w=1}^{4}\left(P_{total}(H_{los}(0) + P_{total}\sum_{ref=1}^{4} H_{ref}(0)\right) + \sum_{n=1}^{4}\left(P_{total}(H_{los}(0) + P_{total}\sum_{ref=1}^{4} H_{ref}(0)\right) + \sum_{p=1}^{1}\left(P_{total}(H_{los}(0) + P_{total}\sum_{ref=1}^{4} H_{ref}(0)\right) \quad . \ . \ . \quad (11)$$

The received power P_r in eqn. (11) is due to each receiver in the receiving plane. Since there is an array of 25×25 receivers in the plane, overall total power P_o can be computed as;

$$P_o = \sum_{1}^{25\times25} P_r = \sum_{1}^{625} P_r \quad . \ . \ . \quad (12)$$

The average received power P_{avg} in the receiving plane is given by P_o dividing total number of planes;

$$P_{avg} = \frac{P_o}{625} = \frac{\sum_{1}^{625} P_r}{625} \quad . \ . \ . \quad (13)$$

If P_{rmin} is the minimum received power in the receiving plane and P_{rmax} is the maximum received power in the plane, then power gap P_g given by;

$$P_g = P_{rmax} - P_{rmin} \quad . \ . \ . \quad (14)$$

The received power distribution uniformity ratio P_{ru} is given by;

$$P_{ru} = \frac{P_{rmin}}{P_{avg}} \quad \text{or}$$

$$P_{ru} = \frac{P_{rmin}}{P_{avg}} \times 100\% \quad . \ . \ . \quad (15)$$

P_g and P_{ru} are the 2 key indicators of improvement in received power distribution.

4. RESULTS AND DISCUSSION

The results of this work were obtained via simulation on MATLB r2018a. The simulation parameters used are listed in table 1**.**

Table 1: Simulation Parameters

1.	Transmitted power	20mW
2.	Transmitter Half power angle	$\Phi_{\frac{1}{2}}$ =70
3.	Receiver/detector FOV	ψ_c =70
4.	Room size	$5m \times 5m \times 3m$
5.	Receiver height	0.85m
6.	Number of LEDs per source	40 × 40
7.	Receiver (receiving plane)	25 × 25
8.	Area of detector	0.0001m^2
9.	Reflectivity of wall	0.8

However, a reduced half angle distribution ($\Phi_{1/2}$ = 4.5°) is first simulated to show the transmitter positions.

Figure 6 depicts the received power distribution for conventional configuration.

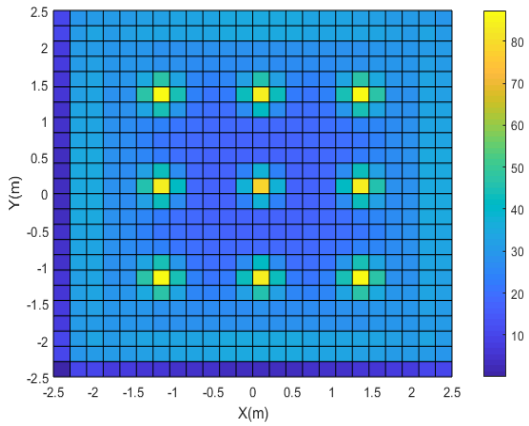

***Figure 6**:* Reduced half angle distribution for conventional configuration

The colour bar indicates the various levels of received power. The distribution of received power observed was poor with a wide gap between maximum (87.3mW) and minimum power (0.074mW). Most of the power happens to be concentrated in areas of the room directly under the transmitters which leads to a high maximum received power. It is these areas that are denoted by 9 clear received power peaks corresponding to the configuration as in *figure 4*. There is also clearly a wide gap between maximum and minimum power because of the very low transmitter half angle that was used which gives the beam of light a very narrow spread making it unable to reach larger portion of the room with strong power.

The case of the novel transmitter configuration is shown in *figure 7* where there is also poor distribution and 9 distinct peaks are also observable which conforms to the novel transmitter configuration as presented in *figure 5*. The results were obtained using the VLC system model, the novel transmitter configuration and received power equations of section 3 and the simulation parameters from table 1. The colour bar in *figure 5* indicates the various levels of power attained in the room from the simulations. The maximum received power was found to be 89.4mW and the minimum received power was obtained as 0.2332mW in the simulation where the novel transmitter configuration was used, which indicates a large gap due to the use of very low half power angle. A high maximum power was also attained because the light was heavily concentrated to small portions of the room.

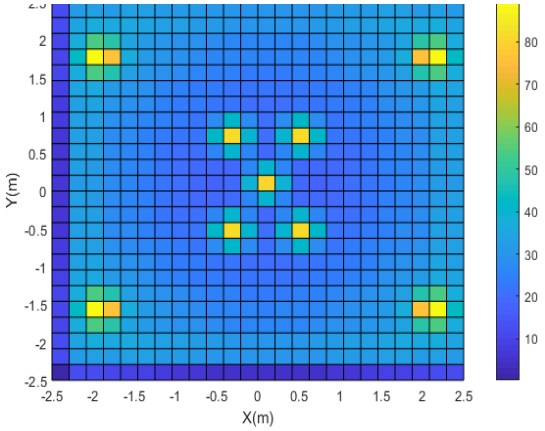

***Figure 7**:* Reduced half angle distribution for the novel configuration

The result for the received power distribution of the full simulation for the conventional configuration is depicted in *figure 8,* here the half power angle was changed back to the original value of 70° in table 1. The colour bar shows the various levels of received power in the room at different points of the receiving plane. The results were obtained using the VLC system model, transmitter arrangement, received power equations of section 3 and parameters of table 1. The peak power obtained from the simulation is $2.3840\,mW$ while a minimum received power of $0.4937\,mW$ was obtained, the uniformity of distribution in this case was obtained to be 0.32 or (32%) distribution using eqn. (15) in the simulations. A power gap of $1.8903\,mW$ was obtained using eqn. (14) in the simulations.

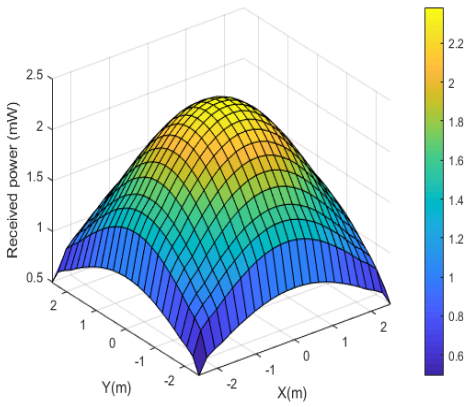

***Figure 8**:* Received power distribution for the conventional configuration

The result of received power distribution for the novel transmitter configuration model presented in this work is shown in *figure 9*.

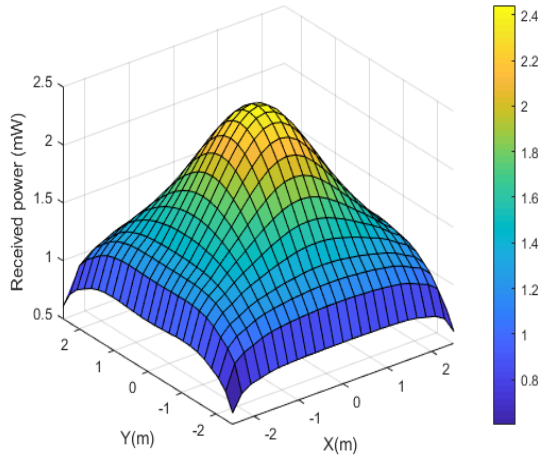

Figure 9: Received power distribution for the novel configuration model

The results were obtained using the simulation parameters of table 1 on a VLC system model as given in section 3. The transmitter configuration used in the simulation is the novel configuration. The colour bar in *figure 9* shows the various levels of received power in the room. The maximum received power during the simulation was obtained as $2.4425\,mW$, while a minimum received power of $0.6016\,mW$ was achieved. A power gap of $1.8409\,mW$ was achieved using eqn. (14) in the simulations and the uniformity of received power distribution was obtained as 0.41 or (41%) distribution using eqn. (15) in simulation. These values were attained as the arrangement offers a good spread of transmitters, the 2×2 wide transmitters give the arrangement a good distribution and a high minimum received power. The narrow 2×2 arrangement offers a good contribution to both the distribution uniformity and also the peak power attainable. While the central transmitter in this novel configuration boosts the maximum or peak received power of the system to the receivers in the center of the plane to ensure it remains high despite the goal of improving the distribution. Due to the varying approach in this work, the evenness of the received power in this case is shown by the spread of the blue colour shades in *figure 9* rather than yellow colour shades as seen from the results of the conventional configuration and most other power distribution improvement schemes.

The result of this novel configuration is presented alongside that of the conventional 9 transmitter configuration in table 2 to clearly have a comparison of their different attained values for different parameters. The values were obtained in simulation using received power equations in section 3.4.

Table 2: Conventional vs Novel Arrangement of 9 Transmitters

s/n	Transmitter configuration	Maximum power P_{rmax} (mW)	Minimum power P_{rmin} (mW)	Power gap P_g (mW)	Overall power P_o (mW)	Average power P_{avg} (mW)	Received Power Distribution P_{ru}
1.	Conventional configuration model	2.3840	0.4937	1.8903	964.19	1.5436	0.32 or (32%)
2.	Novel configuration model	2.4425	0.6016	1.8409	910.21	1.4563	0.41 or (41%)

From table 2, it can be seen that the novel 9 transmitter configuration has better values for the 2 key parameters identified to indicate improvement in uniformity of distribution, that is the uniformity of distribution index P_{ru} and the power gap in the receiving plane P_g. The maximum received power P_{rmax} was also not traded off for the improvement in distribution, it was rather improved as well at room center since there is high probability of having receiver there for an office environment. Hence, this novel arrangement for 9 transmitters can be adopted as better arrangement than the conventional 9 transmitter configuration because, using plural same transmitters which implies same number of transmitters, transmitted power, transmitter and receiver parameters all being maintained, the received power distribution has been improved by 9% (from 32% of conventional configuration to 41% of the novel configuration). This was also achieved not at the cost of maximum power but rather at the same time, a higher maximum power was even obtained. Mobility has been improved also due to less power fluctuation as observed from the less power gap and the novel configuration still maintains an architecturally friendly

setting and design thereby catering for the aesthetics as the lightings are primarily for illumination.

5. CONCLUSION

Received power distribution of an indoor visible light communication system has been modeled and simulated and the results have shown that the novel 9 transmitter configuration introduced in this work has a better distribution than the conventional 9 transmitter configuration by 9% improvement and should be adopted from the viewpoint of better power distribution without trading off peak received power.

The recommendations for future works regarding this research include looking into the aspect of R.M.S delay spread together with maximum achievable data rate, this will give an idea on the effect of the multipath propagation as a result of this novel 9 transmitter configuration. These can be related to the conventional 9 transmitter configuration for further comparison and analysis. On a broader scale, an entirely different configuration for 9 transmitters can be explored and its performance compared with the conventional configuration and also the configuration presented in this work within the limits of the same performance metrics.

REFERENCES

Abdelrahman, S.E. and Abdulwahab, M.M. (2019). Enhancing of SNR and Optical Power Distribution in Indoor Visible Light Communications Systems. *Journal of Telecommunication, Electronic and Computer Engineering,* Vol. 11, No. 3, pp. 23-26. https://jtec.utem.edu.my/jtec/article/view/5210

Cheng, L., Viriyasitavat, W., Boban, M., and Tsai H. (2018). Comparison of Radio Frequency and Visible Light Propagation Channels for Vehicular Communications. *IEEE Access*, No. 6, pp. 2634-2644. https://dx.doi.org/10.1109/ACCESS.2017.2784620

Chvojka, P., Zvanovec, S., Haigh. P.A. and Ghassemlooy Z. (2015). Channel Characteristics of Visible Light Communications Within Dynamic Indoor Environment. *Journal of Lightwave Technology*, Vol. 33, No. 9, pp. 1719-1725. https://ieeexplore.ieee.org/document/7029002

CISCO. (2020). *CISCO Annual Internet Report (2018–2023) White Paper*. https://www.cisco.com/c/en/us/solutions/collateral/executive-perspectives/annual-internet-report/white-paper-c11-741490.html

Dawoud, D.W., Héliot, F., Imran, M.A., and Tafazolli, R. (2020). A Novel Unipolar Transmission Scheme for Visible Light Communication. *IEEE Transactions on Communications*, Vol. 68, No. 4, pp. 2426-2437. https://doi.org/10.1109/TCOMM.2019.2963377

Gismalla, M.S.M., Abdullah, M.F.L., Niass, M.I., Das, B. and Mabrouk, W.A. (2020). Improve Uniformity for an Indoor Visible Light Communication System. *International Journal of Communication Systems,* Vol. 33, No. 8. https://doi.org/10.1002/dac.4349

Gismalla, M.S.M. and Abdullah M.F.L. (2019). Optimization of Received Power and SNR For an Indoor Attocells Network in Visible Light Communication. *Journal of Communications,* Vol. 14, No. 1, pp. 64-69. http://dx.doi.org/10.12720/jcm.14.1.64-69

Khalifeh, A.F., AlFasfous, N., Theodory, R., Giha, S. and Darabkh, K.A. (2019). On the Effect of Light Emitting Diodes Positions on The Performance of an Indoor Visible Light Communication System. *2019 IEEE Conference of Russian Young Researchers in Electrical and Electronic Engineering (EIConRus)*, Saint Petersburg and Moscow, Russia , 28-31 *January, 2019.* https://dx.doi.org/10.1109/EIConRus.2019.8656890

Lee, C.G. (2011). Visible Light Communication, Advanced Trends in Wireless Communications. *InTechOpen*, pp. 327-338. http://dx.doi.org/10.5772/16034

Madani, F., Baghersalimi, G., and Ghassemlooy Z. (2017). Effect of Transmitter and Receiver Parameters on The Output Signal To Noise Ratio in Visible Light Communications. *2017 Iranian Conference on Electrical Engineering (ICEE),* Tehran, Iran, 2017. pp. 2111-2116. https://ieeexplore.ieee.org/document/7985410

Mulyawan, R., Gomez, A., Chun, H., Rajbhandari, S., Manousiadis, P.P., Vithanage, D.A., Faulkner, G., Turnbull, G.A., Samuel, I.F.D., Collins, S. and O'Brien, D. (2017). A Comparative Study of Optical Concentrators for Visible Light Communications. *Proceedings SPIE 10128, Broadband Access Communication Technologies XI, 101280L, SPIE OPTO,* S.A, California, United States, January 28, 2017. https://doi.org/10.1117/12.2252355

Shaaban, R. and Faruque, S. (2020). Optimized LEDs Positions for Channel Analysis Performance of An Intra-Vehicle Visible Light Communication System. *2020 IEEE Radio and Wireless Symposium (RWS),* San Antonio, TX, USA, 26-29 January, 2020 https://dx.doi.org/10.1109/RWS45077.2020.9050056

Sekaran, C.R., Muthuramalingam, A., and Yuvaraj, N. (2022). Transmitter Half Distribution Angle Optimisation in Non-Line of Sight Visible Light Communication. *Journal of Nanoelectronics and Optoelectronics*, Vol. 17, No. 2, pp. 257-266. https://doi.org/10.1166/jno.2022.3192

Slaiman, I., Hisham, N., Hamid, B. and Boon, T.T. (2014). Optical Wireless Communications Through Visible Light LEDs: An Overview. *International Journal of Engineering Research & Technology (IJERT),* Vol. 3, No. 3, pp. 1152-1156. https://www.ijert.org/optical-wireless-communications-through-visible-light-leds-an-overview

Vatansever, Z., and M Brandt-Pearce, M. (2017). Visible Light Positioning With Diffusing Lamps Using an Extended Kalman Filter. *2017 IEEE Wireless Communications and Networking Conference (WCNC),* San Francisco, CA, USA, 19-22 March, 2017. https://dx.doi.org/10.1109/WCNC.2017.7925652

Wang, W.C., Chow, C., Wei, L Y., Liu, Y. andYeh, C. (2017). Long Distance Non-Line-of-Sight (NLOS) Visible Light Signal Detection Based on Rolling-Shutter Patterning of Mobile-Phone Camera. *Optical Society of America, Optics Express (10103-10108) Research Article*, Vol. 25, No. 9. https://doi.org/10.1364/OE.25.010103

Yu, Z., Baxley, R.J. and Zhou, G.T. (2013). Multi-User MISO Broadcasting For Indoor Visible Light Communication. *2013 IEEE International Conference on Acoustics, Speech and Signal Processing,* Vancouver, BC, Canada, 26-31 May, 2013. https://dx.doi.org/10.1109/ICASSP.2013.6638582